DELIVERABLE 2.2
Implementation and performance evaluation of the prototype Olive fruit fly detector

Project Acronym	**ENTOMATIC**
Project Reference:	**605073**
Project Title:	**Novel automatic and stand-alone integrated pest management tool for remote count and bioacoustic identification of the Olive Fly (*Batrocera oleae*) in the field**

DELIVERABLE 2.2 - Implementation and performance evaluation of the prototype Olive fruit fly detector

Revision: v0.1

Authors:

TEIC: Ilias Potamitis, Panagiotis Eliopoulos, Charalampos Manifavas, Nicolas Alexander Tatlas, Dimitris Kontodimas, Efthymios Bakarezos, Sofia Boudouridou, Giota Psirofonia, Ioannis Sarantopoulos, Vasileia Boura, Elias Chrysocheris, Vasilis Dimitriou, Vasilis Samaritakis, George Tentes, Konstantinos Sakkas, Dimitra Christopoulou, Ioannis Kapetanakis, Charalampos Papadakos, Eleftherios Alyssandrakis, Angelos Chaidas

Received input/comments from:
AJAJP: Joao Mira
PHYTO: Stavrakis Nikos
BIOSYS: Guy De Laude
IMMS: Frank Spiller
AVIA-GIS: Ward Bryssinckx
UPF: Albert Bel Pereira

Project co-funded by the European Commission within the ICT Policy Support Programme		
Dissemination Level		
P	**Public**	**X**
C	**Confidential, only for members of the consortium and the Commission Services**	

Revision History

Revision	Date	Author	Organisation	Description
1	17/12/2016	TEIC	TEIC	V0.1_rev12
2	27/12/2016	TEIC	TEIC	Amendments and comments
3				
4				
5				

Statement of originality:

This deliverable contains original unpublished work except where clearly indicated otherwise. Acknowledgement of previously published material and of the work of others has been made through appropriate citation, quotation or both.

TABLE OF CONTENTS

LIST OF TABLES

LIST OF FIGURES

1 INTRODUCTION

This Deliverable presents our most recent results on an electronic trap for automated monitoring of insect populations of fruit flies. Diptera of the Tephritidae family are fruit flies that each year effect a crop loss calculated in billions of euros worldwide [1]. Female *Bactrocera oleae* (Gmelin), *Ceratitis capitata* (Widemann), and *Bactrocera Dorsalis* (Hendel), among many others, demonstrate high reproductive rates. These pests lay eggs beneath the fruit surface, the eggs hatch and larvae feed inside the fruit. As a result, the fruit drops or its quality degrades. Pests can be controlled with ground pesticide sprays or biological means, the efficiency of which depends on knowing the time, location and extent of infestations as early as possible. The decision on when to begin treatment is based on manual crop scouting. Insect traps attract the pest using chemical signals that originate from pheromone or food baits placed inside the trap. The network of monitoring traps is composed of tens to hundreds of traps and, in large orchards, can be dispersed to many miles among nodes.

Automatic monitoring of pests in agricultural crops in the context of our work for this Deliverable intends to provide the following services:

a) Increased productivity due to timely delivery of comprehensive information to a central agency. The central agency receives information on location and density of the targeted pest as well as parameters of the microclimate. This information can be used to alert for the presence of the pest and serve as supportive evidence to initiate the treatment procedure. The onset of an infestation is a crucial parameter that is often missed in manual inspections as it may fall between scheduled manual visits. The Economic Injury Level for *B. oleae* is 5–20 *B. oleae* found per trap for 5 days period. Economic Injury Level in pest management means that if you miss this point then economic damage begins and for the case of this pest it can be large.

b) Time-stamping of the event of insect entrance in the trap allows the gathering of precise information on the life cycle of the pests and their relation with different pheromone and/or food baits. Moreover, it allows continuous and real-time evaluation of the results of applied treatments. The central monitoring agency securely reflects the current situation of the infestation and not a situation that has evolved to an unknown state due to delays in the delivery and interpretation of the relevant information.

c) Reduction on the application of pesticides and increase of their applied efficiency. Cultivators often start too early or overspray in fear of missing the infestation onset. Knowledge of where and when to apply a treatment can mitigate the problem of over-application of pesticides in one region and under-application in another.

d) Increase the profit margin by decreasing the current labour-intensive and expensive manual monitoring activities. Current manual inspection involves field scouters visiting a remote network of traps on a regular basis. This procedure entails a time lag between the phenomenon and its report, and increases the cost due to transportation expenses and wages.

e) For countries, where production of fruits is a countable percentage of their total gross income, monitoring and control is handled by the state, while agricultural unions and large orchard owners can take further actions. Once the trap is located, the human observer must discern and count the targeted pests. This is not always feasible as these may have disintegrated or be obscured in the maze of insects. This practice is a complicated procedure that involves open tenders, contracts, qualified personnel working at different report layers. Because of the number and location of the traps, the frequent trips and the expertise required, the requirements of the monitoring protocol are compromised in practice, as one may judge from the large reported losses due to Diptera infestations.

The penetration of high-end technology into the automated identification of insects and possibly control of pests has made its appearance and is gaining solid ground [2-4] but is far from being considered established in view of practical applications adopted by cultivators. In

[5-10] researchers have been trying to sense the presence of a targeted pest and report its counts for various insects of interest. The vast majority of reported cases treat the insect as a falling body that causes photo-interruption which leads to a binary decision and counting. In [10] we presented a novel approach where the pest is counted and classified according to its wingbeat. In the light of further progress reported in [11-12] this Deliverable focuses on facing all deficiencies encountered in [10]: it is more accurate, power efficient and practical, as we introduce several distinct novelties in the construction of sensors and electronics to shift the research on this device from good science to good practice. In detail:

a) The receiving aperture of the sensor is made large enough to allow tracking of fast flying insects such as fruit flies that would otherwise spend little time inside the field of view (FOV) while crossing the surface of a single photodiode. Lack of sufficient duration data is translated into poor frequency resolution for fast flying insects such as fruit flies.

b) Our boards were redesigned based on low-power electronics and optimized software to maintain power consumption at a sufficiently low level in order to be able to operate the device in the field for at least two months without the need of a solar panel.

c) New algorithmic design based on interrupt-driven circular buffers never misses the onset of the wingbeat, even when it occurs before the initialization of the recording process.

In the near future, provided that automated monitoring will reach large scale deployment of monitoring nodes, the correlation of insect counts with such environmental parameters as humidity, temperature and GPS coordinates will allow the prediction of food productivity and prices using statistical predictive modelling. Moreover, transmitted results can be correlated and co-interpreted along with the general state and changes of the climate. Prediction of future infestation outbreaks based on historical data will also be feasible. Finally, the traps can serve as beacons summoning and guiding unmanned flying vehicles (drones) to spray only in designated areas. Therefore, for large agricultural areas the repetitive circle of treatment with spraying drones and after-treatment assessment with e-traps can be automatized to a great extent.

2 MATERIALS AND METHODS

2.1 INTERNAL CONFIGURATION

The device is designed so as to introduce the minimal disturbance into the internal space of a McPhail type trap. We build on traps that have been proven in time to be compatible with the life cycle of insects as we did not want a new design to jeopardize the effectiveness of the trap in attracting insects. Therefore, all electronics are gathered in a slim 2.75 cm thick add-on component attached from the outside on the top of the trap (see Fig. 1-Left), and all plastic parts are made transparent. The size of the electronics, compared to [10], is halved without any compromise in the processing capabilities or its cost. All cables are directed inside and through the supporting tubes that also serve as holders of the sensor which guards the entrance to the trap. There is an intentional gap between the internal border of the inverted funnel and the holder of the sensor as fruit flies may enter in two ways: either directly flying-in or landing outside, walking to the inner border and then flying in as there is no other way to enter the trap. The insects follow the high concentration of odors at the top of the trap due to bait evaporation that is placed at the bottom and stick to the walls of the trap as these are better illuminated than the interior. The trapped insects finally fall in the bait out of exhaustion or because the bait contains detergent that evaporates along with it. Note that the reverse motion of flying out is atypical for the flight patterns of the fruit-fly (see video supplement) and the shields around the sensor protect the sensor from double counting. Regarding the optical sensor seen in Fig. 1-right, as introduced in [12], we use a lightguide as a receiver and an array of infrared LEDs with an attached diffuser as an emitter (see Fig. 1). A 1D linear array as well a 2D array of photodiodes proved insufficient for flying insects such as fruit flies, as their fast movement and relatively low wingbeat frequency did not leave enough traces for their efficient identification. Note that the photodiodes we use have 3.5 mm width and the gaps between them effected a variation in the intensity of received light as the fruit fly crossed the diode in less than 30 ms. The lightguide having a wide receptive area of 7.2x2.3 cm^2 has solved all problems of this kind and delivers an average 100 ms of wingbeat recordings. The lightguide is made of parts of laptop screen sheets and is used in reverse functionality.

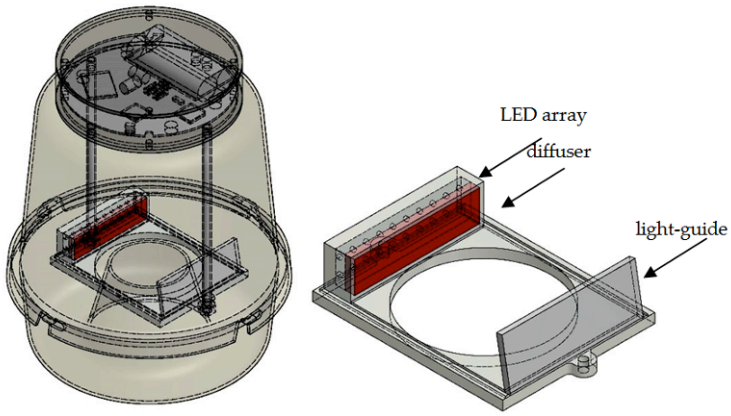

Figure 1: (Left) Schematic diagram of the automated monitoring trap. (Right) Enlarged detail of the optical sensor

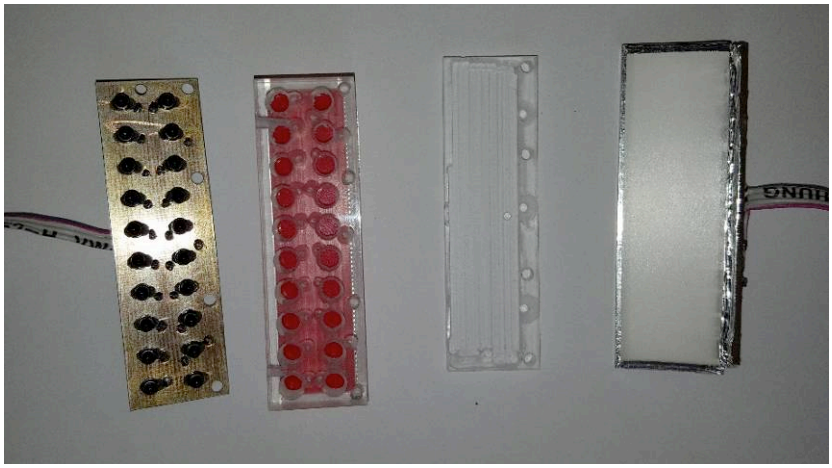

Emitter: LED array (left), diffuser (right) Receiver: polarizer and light-guide

Figure 2: Sensor. First two items on the left compose the emitter and the rest two on the right, the receiver.

In laptop screens the light is directed from the motherboard up the screen and out whereas, in our case, the infrared light from the emitter placed at the opposite to the lightguide is directed down to the base of the screen where it is collected by a 1D array of photodiodes attached to one edge of the lightguide.

Diffusers and polarizers (see Fig. 2) are commonly used in thin-film transistor, laptop screens. In the context of our work for this Deliverable, the diffuser is used so that the lightguide sees a smooth light distribution of almost equal intensity, stemming from a rectangular array of the LED array. The polarizer improves the SNR of the signal in the receiver by almost 3dB. The waveguide and polarizer are similar to these used in laptop screens (type LTN154U2-L03).

The number of LEDs was defined by a trial and error procedure. Fewer LEDs lead to areas with higher light intensity than others. This results to variations in received signal power as a fast insect passes from the lighter to the less illuminated spot and back. This is more visible when one also employs 2D arrays of photodiodes. To secure that the receiver senses the same light intensity at the borders, the LEDs around the borders are driven with higher current than the central ones as otherwise the receiver would receive a greater intensity of infrared light in its center. Currently, the plastic trap is covered with a sun-blocking film that allows visible light to enter the trap but, according to the specifications, it rejects 97% of infrared radiation at 900-1000 nm (3M Crystalline CR70).

2.2 ELECTRONICS

The trap is designed to be operated in the field without a constant power source. The main issue of concern during development was to implement a device with as low power consumption as possible. Because of limited power resources one has to set priorities on performed tasks and algorithmic complexity. First, we give details on the power consumption plan and how this can last up to the desired level: We used a MSP432P401R microprocessor (MCU) to carry out all tasks, from sending pulses

through the emitter and monitoring the light intensity at the receiver to matching patterns and delivering data through the GPS-GRPS card (see Appendix for details). Power consumption totals to 9.57mW from which 4.3mW are consumed on the analogue part of the device (LEDs 4.29 mW, photodiodes amplifier 10uW) and 5.28 mW on the digital part (MCU 4.95 mW, SD 0.33 mW). The device is powered by two batteries (2x3000 mAh) and when following a report schedule of once per day and a typical case of 10 triggers per day the device is power sufficient for 60 days.
The clock of the MCU instructs the emitter to send high energy pulses of 200 mA with duration of 1.6 microsecond every 250 microseconds. Pulses are transmitted and received in accordance to the clock. The synchronization pulses are produced by the embedded timer of the MCU in capture/compare blocks. The duration of the pulses has been defined from the response time of the photodiodes (500nSec). Hereinafter, we describe a period of 250 uSec (see Fig. 3):

1. ADC process and data storage
2. After 24 uSec, enable receiver
3. At 1100nSec, emit a 1.6 uS pulse
4. At 800 nSec, Sample – Hold for 800nSec
5. De-activate emitter, de-activate receiver.

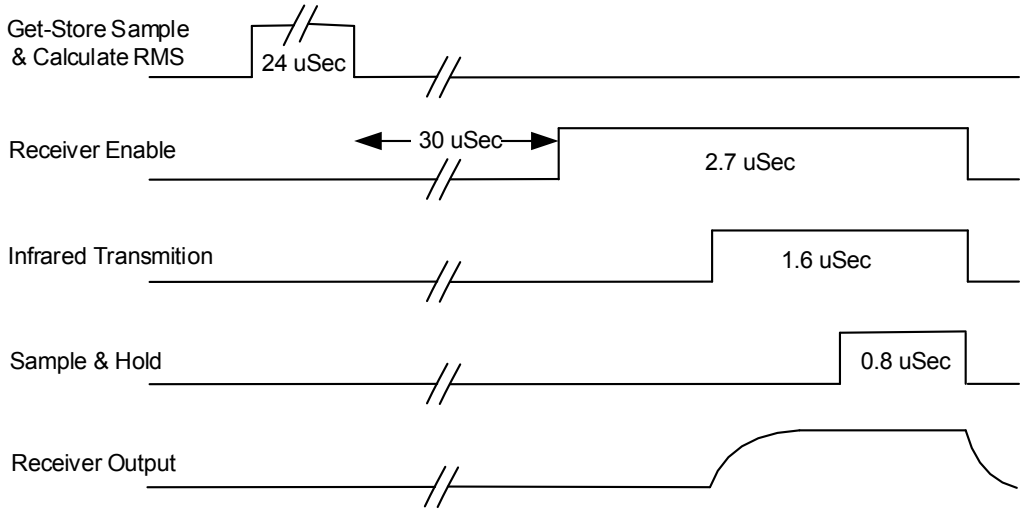

Figure 3: Synchronization diagram between emitter and receiver. The process is repeated every 250 uS. MCU is active only during the Store Sample & Calculate RMS step.

The output signal from the receiver is driven to a sample & hold circuit. Subsequently, it is driven through AC-coupling to an amplifier so that one amplifies the useful signal, and then to the embedded ADC of the processor.

The intermittent light transmission allows us to send high energy pulses that are useful to illuminate the wings, at the same time saving a considerable amount of power, as it is active for a limited time. Non-continuous light is the key to low-power operation. Note, that no solar cell is required and the device can last longer if it is switched off at night as *B. oleae* is only active in daylight. The SIM is always in sleep-mode. It is woken up by the MCU on a prescheduled basis, transmits and is switched off again. During SIM activation-transmission all other signal processing procedures are halted to avoid electromagnetic interference. Transmission takes place at night when *B. oleae* is inactive; therefore, no loss of wingbeat events of the target pest are possible.

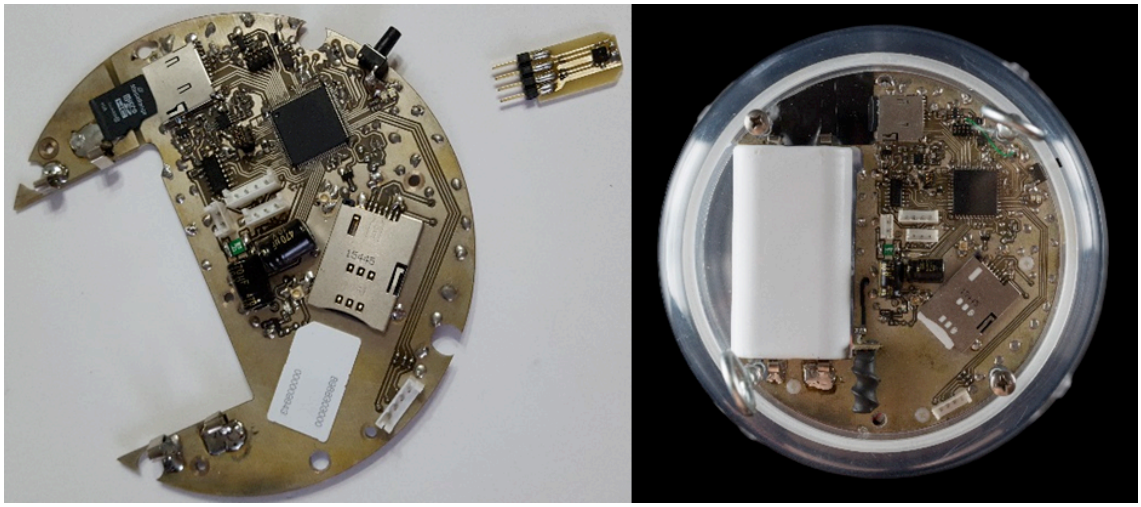

Figure 4: (LEFT) The electronic board of the automated fruit fly trap. (RIGHT) Final placement of the board in the trap

The SNR than can be achieved by a 14 BIT ADC is in theory approximately 86dB. The 14 bit depth of the embedded ADC of the processor is enough to code the analogue signal of the receiver as the noise level of our system is -75dB. Therefore quantization noise is lower than the produced noise.

2.3 CODE

The embedded microprocessor runs a constantly-looping program which processes the data captured by the optical sensor. The board (Fig. 4) is programmed in optimized C/C++. The MCU executes two basic procedures: The first one is interrupt-driven and stores the ADC data in a cyclic buffer of 16K samples, that is, the line-level output from the optoelectronic sensor is copied to a circular buffer. The same procedure monitors the signal's root-mean-square (RMS) using a window of 128 samples (16 ms in 4 kHz sampling rate). If the RMS of the window exceeds a predefined threshold, an event has been detected, i.e. an insect has crossed the sensor's FOV. This triggers the recording of the signal capturing 1024 samples of 256 ms duration from the second cyclic buffer coded with 14-bit resolution, at 4 kHz sampling rate. There is no further processing or storage prior to the triggering event excluding the circular buffer. After triggering, 200 samples (i.e. 50 ms) are drawn before and up to the triggering point and 824 samples (i.e. 206 ms) after that point in order to ensure that the onset of a wingbeat event is not lost. The low sampling frequency is enough to sample the wingbeat frequency of fruit flies expected around 200 Hz and several of its partials as well. Wingbeat events are short in time for fast flying insects such as flies and one cannot afford discarding any useful part of the signal such as the onset. The sampling frequency, window length and triggering threshold are pre-stored in the SD-card and are read once during powering-on of the device. After triggering, the subsequent performed tasks are: a) Fast Fourier Transform (FFT) of the data chunk captured, b) decision on the identity of the insect based on analysing its wingbeat and c) storing the wingbeat snippet in the SD card and queuing information to be transmitted on a pre-scheduled basis to a server. If during the FFT process we have a new event this will be stored in the main 16K buffer and will be served when the MCU completes the previous event. When there is no trigger, all MCU procedures but the window monitoring the RMS level rests in sleep mode.

The exact duration of processing stages in analysed in Table 1:

Process	Time (ms)
Collect data	200
Copy data to buffer	800 uS
4xFFT (256 points)	7
Log_{10}	800 uS
Decision	1.2
Store in SD	60
Total	269.8mS

Table 1: Timing of events in CPU

3 RESULTS

The triggering stage results to a data chunk of 1024 samples holding only the wingbeat event. In Fig. 6 we show examples of the wingbeat events. There is a slow varying in time amplitude part (see Fig. 5-left), almost non-oscillatory, which is due to the main body movement that appears at low frequencies near DC in Fig. 5–right. We would get the same slowly varying pattern with a simple drop of an object through the FOV. On the slow varying part one can clearly see the imposed oscillatory contribution due to the modulation that the wingbeat inflicts on the light intensity. The power spectral density (PSD) one-sided estimate of each snippet is found by splitting the waveform in 4-chunks of 256 samples each without overlapping. The modified periodogram is computed using a Hamming window of 256 samples followed by a 256 points Discrete Fourier Transform (DFT). The DFT's are averaged and log-transformed to obtain the PSD estimate of the recording. In Fig. 5 we line-up several wingbeat recordings from different *B.oleae* individuals taken from the trap in operational mode and stored in the embedded SD. The SNR is around 50 dB calculated as:

$$SNR = 20 * log\left(\frac{Signal\_RMS}{Noise\_RMS}\right) \quad (1)$$

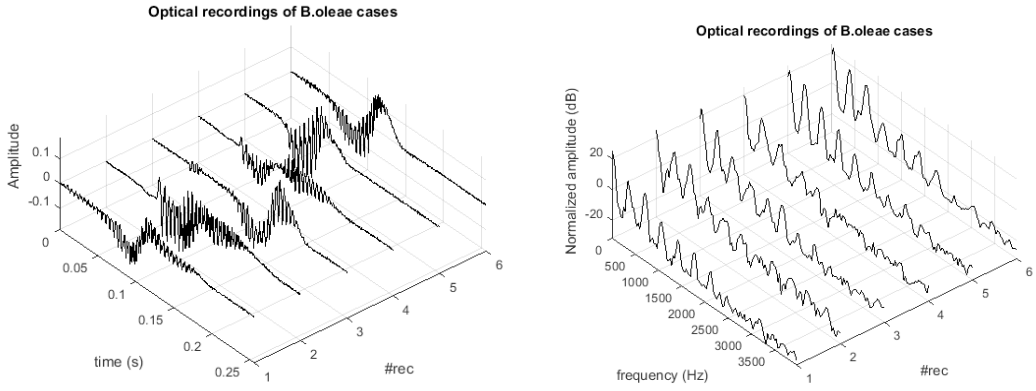

Figure 5: (Left) Optical recording of different cases of *B. oleae* flying in the trap. High-frequency modulation due to wingbeat and low-frequency main-body movement. (Right) Spectrum of the corresponding recordings. The fundamental frequency is at around 200 Hz and at least 5 harmonics are resolved

We use the frequency content of the wingbeat as biometric evidence for species classification. Note that, besides the fundamental frequency, information bearing parts of the signal are the exact location of the partials (some higher partials can be detuned from the exact placement of harmonics), the distribution of energy on the harmonics, the amplitude of the near-DC frequency content related to body-size and the way spectral leakage is distributed around the partials.

3.1 VERIFICATION RESULTS IN THE LAB

Verification involves answering a problem with a binary answer: once the device (Fig. 7) is triggered, due to a detected insect entering, the question is whether it was *the target species (i.e. B. oleae in our case) that flew in or not*. We are not interested in the context of this Deliverable to recognize any other species other than the target pest. Two approaches were examined: a) a simple, rule-based approach that reports results based on calculations carried out inside the trap, and b) results based on analyzing off-line the stored recordings. The first approach is based on two simple rules that simultaneously must hold in order to count a signal as a target case: *Rule 1*: Examine if the amplitude of the time domain recording is within the limits derived from a large number of *B. oleae* recordings (see Fig. 6). Insects that have larger wings than *B. oleae* will return a larger fluctuation on signal amplitude and, on the contrary, insects that are much smaller (e.g. midges) modulate light at much smaller amplitudes. *Rule 2*: Examine the frequencies between 170 and 230 Hz where the fundamental frequency of *B. oleae's* wingbeat lies and if the energy of this bandwidth exceeds a threshold then call it a verified detection. Thresholds are derived from positive examples in the lab. The rule is simple and efficient provided there are no competing fruit-flies in the olive orchard. This rule cannot, by default, tell the difference between *B. oleae, C. capitata* and *Lonchaea aristella* (Diptera: Lonchaeidae) whose spectra totally overlap (see Fig. 6). However, it rejects 80% of Drosophila cases and 100% of all mosquitos' cases we tried. Drosophila is a smaller insect compared to *B. oleae* and beats its wings at higher frequencies between 260-310 Hz and mosquitoes have an even higher fundamental frequency when all are observed in the same reference temperature. We never observed triggering of the device in the absence of an insect flying in. Similarly, the device is immune to insects walking without flapping their wings.

We then focused on employing more complex and computationally involved algorithms that currently can be carried out on a server to examine the full information quality of the wingbeat. In practice this would entail the transmission of the snippet from the SD of the trap to the server. All recordings in Table 2 are taken by insects that either flew in from the container to the trap or landed on the outside of the inverted funnel entrance, walked inside up to the border that they tend to explore by walking and then flew in (see Fig. 7). No attractant was used other than physical light and random variation in temperature and humidity was kept as low as possible.

Insect	#rec
B. oleae	913
C. capitata	623
Drosophila+	166
L. aristella	771
Total	2473

+Genus *Drosophila*, species unidentified.

Table 2: Dataset composition

One should note that this is a challenging dataset reflecting a worst case scenario in reality as it investigates the possibility of discerning a specific fruit fly among other fruit flies only from its wingbeat.

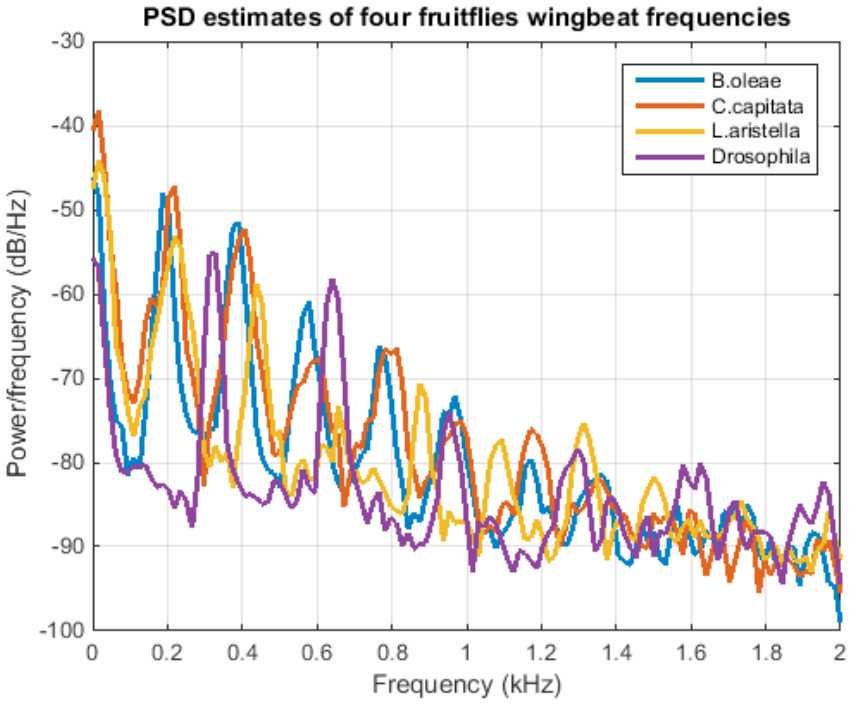

Figure 6: (Left) Power Spectral Densities of the wingbeat of four fruit flies. The fundamental and the harmonics overlap significantly

The recorded dataset depicted in Table 2 is based on the experimental setting shown in Fig. 6. All adult insects of all species in the work for this Deliverable started as larvae inside fruits (i.e. olives for *B. oleae*, peaches for *C. capitata* and figs for *L. aristella*) and they feed upon the pulp until they exit, usually as third instar larvae. Then they are collected and grown in an insectary cage. As larvae turn into adult insects, we supply them with yeast hydrolysate-sugar diet and water to sustain them to life. We keep only first generation insects, as breeding generations of insects in captivity results into degeneration that might affect the flying mechanism and our target are insects of the real-field. Each insectary cage contains strictly one species and about 200-300 adults of both sexes.

Figure 7: Testing setup. The trap is fixed on the entrance of a dark tube. Fruit flies are placed inside the tube. Insects follow the light at the end of the tunnel and either fly in the trap directly or most commonly, walk until the internal border of the trap and then fly in.

Classifiers	%mean acc./std
Linear SVC[1]	88.46/1.24
RBF SVM[2]	90.52/0.99
RF[3]	91.05/1.55
ADABOOST	88.62/1.01
X-TREE[4]	91.13/1.21
GBC[5]	91.63/1.31
CNN[6]	90.40/1.18

[1] linear kernel, C=0.01
[2] radian basis function kernel, gamma=0.009, C=0.2
[3, 4] #trees=650, min_samples_split=2, min_samples_leaf=1
[5] min_samples_split=5, min_samples_leaf=30, max_depth=4
[6] SGD optimizer(learn_rate=0.01, decay=1e-4, epochs=60).

Table 3: *B. oleae* verification results. Mean accuracy of top-tier classifiers using a 10-fold cross validation scheme with 20% of the corpus holdout. Verification results of B. oleae (913 cases) against 3 other fruit flies (1560 cases). Note that each species contains both sexes. Mean and standard deviation of accuracy measure over all folds (% mean/std over). Linear SVC: Linear Support Vector Classifier, RBF SVM: Radial Basis Function Support Vector Machine, RF: Random Forests, Adaboost: Adaboost Meta classifier, X-Trees: Extra Randomized Trees, GBC: Gradient boosting Classifier, CNN: 1D 3 layers, Convolutional Neural Network

Adult insects are taken in turn and placed in the black container until they fly in the trap. All *B. oleae* snippets are tagged with label '1' and all others with label '0'. We first assessed the verification performance of popular classifiers based on 10-fold cross-validation. The whole dataset is randomly shuffled, 80% of the dataset is used for training and the rest 20% for testing. The whole procedure is repeated 10 times and the mean accuracy and standard deviation over 10-folds is reported in Table 3. To further elaborate on the recognition accuracy we use precision, recall and F1 score metrics on a random 20% holdout part of the dataset and also derive the confusion matrix of the test set. One should note that in binary classifications there are two sources of errors: the system can fail to classify correctly a target (i.e. a miss) and the system can erroneously classify a fruitfly that is not *B.oleae* as such (i.e. a false alarm). Precision (P) is defined as the number of true positives (Tp) over the number of true positives plus the number of false positives (Fp).

$$P = \frac{T_p}{T_p + F_p} \tag{2}$$

Recall (R) is defined as the number of true positives (Tp) over the number of true positives plus the number of false negatives (Fp).

$$R = \frac{T_p}{T_p + F_n} \tag{3}$$

These quantities are also related to the (F_1) score, which is defined as the harmonic mean of precision and recall.

$$F_1 = \frac{2P*R}{P+R} \tag{4}$$

High precision relates to a low false positive rate, and high recall relates to a low false negative rate. High scores for both show that the classifier is returning accurate results (high precision), as well as returning a majority of all positive results (high recall). We did not try to optimize the feature set as this is not the focus of this Deliverable[1].

We subsequently derive the confusion matrix of a classification model using a single, random peak of a 20% holdout set (see Table 3 and Fig. 6). The confusion matrix, in our case (see also Table 4 and Fig. 8) reveals the extent of misses and false alarms. One can notice the diagonal structure of the confusion matrix indicating that the strong tendency is to classify correctly the species and genera of the flying insect. The results in Table 4 are based on a Random Forest Classifier.

Species	**Random Forest Classifier**			
	precision	**recall**	**F1**	**#rec**
B. oleae	0.96	0.94	0.95	319
All other	0.90	0.92	0.91	176
Avg/total	0.93	0.93	0.93	495

Table 4: Different accuracy metrics using a 20% hold out set

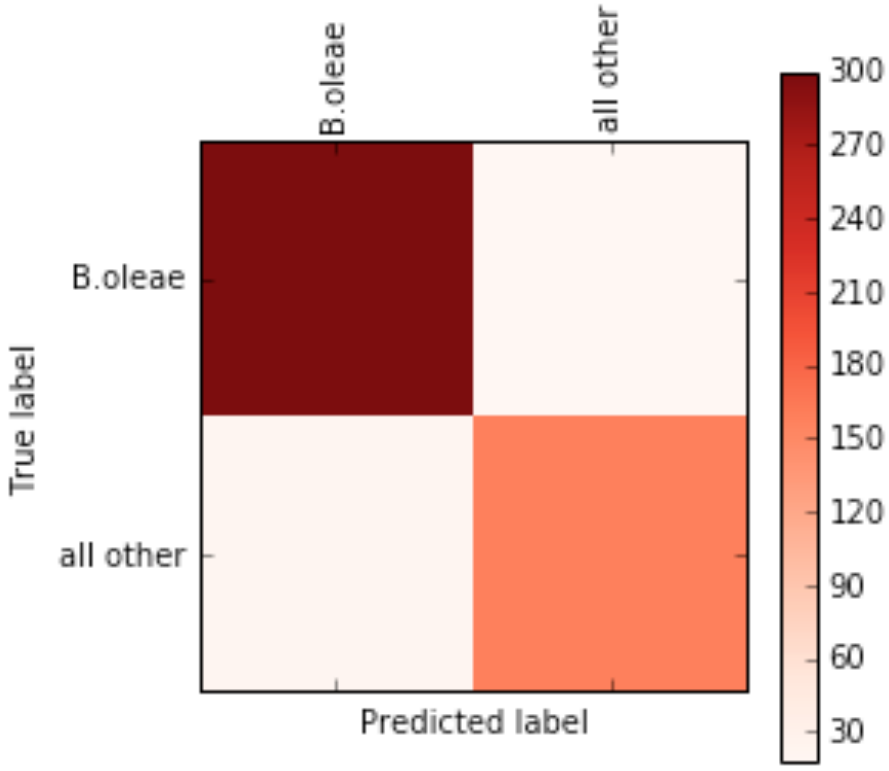

Figure 8: Confusion Matrix on a randomly selected 20% hold out set. Out of 319 cases of B.oleae 300 are classified as such and 19 are misclassified. From 176 cases of non-target fruit flies (i.e. C. capitata, A. lonchaea, Drosophila) 154 cases are correctly classified as non-target whereas 22 cases are False alarms. One can see clearly the diagonal structure of the confusion matrix indicating relatively low confusion rates

[1] In Matlab, feature extraction takes one line of code: c=10log10(pwelch(x,256,192,256,4000)); % Include main body movement

3.2 VERIFICATION RESULTS IN THE FIELD

Large scale experiments in the field are pending. Using only a single prototype, we placed the trap (see Fig 9 for various angles of view) in the field, and left it exposed to the summer sun of Greece while performing several preliminary tests. One should note that the shift from the controlled environment to the field must be made gradually and with care due to the uncontrolled and often unforeseen situations of the exposed field. With the application of the infrared blocking film, the trap did not auto-trigger because of solar radiation even when exposed directly to the mid-day sun that lifted the internal temperature of the trap to 60 ^{o}C. Liquid attractants caused several problems and were replaced with gel-type ones along with vapona stickers insecticide (i.e. Dichlorvos). Careful regulation of the triggering threshold prevents the trap of registering counts due to moving branches and leaves of the trees providing shade to the trap that initially did cause false alarms. The trap is immune to smooth movements e.g. due to a gentle breeze but is vulnerable to abrupt hits or shocks that registered false alarm measurements in a windy day.

Figure 9: (Left): Electronic McPhail trap prototype. Various angles of view

4 DISCUSSION

The experimental results from this Deliverable support the following suggestions: The *in-situ*, rule-based approach has the advantage of being robust against temperature variations. *B. oleae* is active in the range 15-35 ^{o}C and its wingbeat frequency can vary from 160 Hz to 220 Hz in the same temperature range. By including the energy of the whole bandwidth in our calculations of a proper threshold, we can be robust against temperature variations. Based on the need to push the verification accuracy further we examined the possibility of classifying the records using state-of-the-art classifiers that are computational intensive and require the snippets to be transmitted in order to be classified off-line on a server. Note that these recordings were all taken around 30 ^{o}C. In real-time operational conditions one will need classifiers that are immune to wingbeat changes due to temperature variations between 15-35 ^{o}C. We are indeed able to compensate efficiently for the effect of temperature variation but this will not be demonstrated in this Deliverable. One should note that this data set reflects a worst case scenario where all insects flying into the trap are fruit flies and one needs to spot only the *B. oleae*. Still, the results are quite promising reaching a mean accuracy of ~91% (Table 3). The inclusion of the low frequency part due to body movement increased the accuracy by 1%. This is attributed to the fact that different species have morphological differences. All machine learning techniques achieve comparable results and we further elaborated on precision and recall scores (i.e. quantification of the miss and false alarm errors) in Table 4 and in Fig. 8. The offline classification results are very encouraging and suggest that for monitoring application it would be wise to consider the possibility of transmitting 1024 numbers per recording to the tracking site and classify them there and subsequently update the infestation maps of the server. There is room for improving the recognition scores by blending classification models and optimizing the feature extraction process. In order to operate the device in the field we follow two different routes: a) we cover the trap with a semi-transparent infrared blocking film so that the infrared radiation of the sun is blocked from functioning as an emitter and, therefore, projecting any movement outside the trap (e.g. originating from moving tree branches, insects flying outside the trap etc.) to the sensor, b) we investigate low-power versions of modulation/demodulation circuits as in [11] that allow operating without the application of an infrared blocking film.

We suggest that automatic monitoring traps can be used to pinpoint or even predict the onset of infestations and help decision making on properly regulated insecticide application. This technology is more expensive than a typical plastic trap. Note also that, although monitoring helps in taking prevention measures to reduce damage, it cannot enforce eradication of the pest. Therefore, the cost to benefit ratio needs to be calculated objectively and at large scales before automatic monitoring is accepted. The annual losses of this pest can be calculated objectively because they leave a mark on the olive fruits and they increase the acidity of olive oil that can be measured precisely. The losses that are reported annually because of this pest persuades us that automatic monitoring will finally prevail.

5 CONCLUSIONS

Electronic insect traps that monitor insects of economic importance such as fruit flies support the effort to ensure food supplies for a rapidly growing global population. We have demonstrated an autonomous trap that can obtain quality recordings of the wingbeat of flying-in insects, count them, discern species and transmit counts through the mobile network. Species verification can be achieved either in-situ or by transmitting the recordings and performing recognition on a server. As the version of the trap described in this Deliverable does not transmit the recording we derived recognition scores based on the recordings stored in the embedded SD card. When performing a decision in situ on the identity of the incoming insect it can only discern fruit flies against insects with great differences in size and/or spectrum. It cannot tell the difference among fruit flies (e.g. the difference between *B. oleae* and *C. capitata*). However, based on the recordings that are stored inside the trap and with a view to transmitting the recordings, the recognition scores are greatly improved suggesting that transmission of the snippets allow for better discrimination even among fruit flies at the cost of an increased power consumption and decreased algorithmic complexity at the trap level.

Supplementary Materials: The following are available online at https://www.youtube.com/watch?v=IdWVaCyHEVI, Video S1: Automated surveillance of fruit flies.

Acknowledgments: Plastic McPhail type traps and attractants were provided by Phytophyl-N. Stavrakis—Insect Attractants & Insect Traps, Athens, Greece. Mass production of traps has started with the help of IMMS that has printed a 22-25 circuits based on TEIC's electronic diagrams.

6 REFERENCES

1. Oerke, E.C., Dehne, H.W., Schönbeck, F., Weber, A., (1994). Crop Production and Crop Protection: Estimated Losses in Major Food and Cash Crops. Elsevier Science. Amsterdam.
2. V. A. Drake, Radar Entomology, CABI Publishing, 2010, ISBN 10: 184593556X / ISBN 13: 9781845935566
3. A. Gebru, E. Rohwer, P. Neething, and M. Brydegaard, "Investigation of atmospheric insect wing-beat frequencies and iridescence features using a multispectral kHz remote detection system," J. Appl. Remote Sens. 9221, 922106 (2014).
4. Emma R. Mullen, Phillip Rutschman, Nathan Pegram, Joseph M. Patt, John J. Adamczyk, and 3ric Johanson, "Laser system for identification, tracking, and control of flying insects," Opt. Express 24, 11828-11838 (2016).
5. Hendricks DE (1989) Development of an electronic system for detecting Heliothis spp. moths (Lepidoptera: Noctuiidae) and transferring incident information from the field to a computer. J Econ Entomol 82:675–684.
6. Watson, A.T., O'Neill, M.A., and Kitching, I.J. (2003). Automated identication of live moths (macrolepidoptera) using digital automated identication system (daisy). Systematics and Biodiversity, 287300.
7. Jiang Joe-Air, Tseng Chwan-Lu, Lu Fu-Ming, Yang En-Cheng, Wu Zong-Siou, Chen Chia-Pang, et al,. A GSM-based remote wireless automated monitoring system for field information: A case study for ecological monitoring of the oriental fruit fly, Bactrocera dorsalis (Hendel), Computers and Electronics in Agriculture, 2008; 62, 2, 243–259, ISSN 0168-1699, http://dx.doi.org/10.1016/j.compag. 2008.01.005.
8. Holguin, German A.; Lehman, Brian L.; Hull, Larry A.; Clement, Teah; Jones, Vincent P.; Park, Johnny, Electronic traps for automated monitoring of insect populations, Vol. 3, Part 1, pp. 49-54, 3rd IFAC International Conference Agricontrol, 2010.
9. Bromenshenk, J.J.; Henderson, C.B.; Seccomb, R.A.; Welch, P.M.; Debnam, S.E.; Firth, D.R. Bees as Biosensors: Chemosensory Ability, Honey Bee Monitoring Systems, and Emergent Sensor Technologies Derived from the Pollinator Syndrome. Biosensors 2015, 5, 678-711.
10. Potamitis I, Rigakis I, Fysarakis K (2015) Insect Biometrics: Optoacoustic Signal Processing and Its Applications to Remote Monitoring of McPhail Type Traps. PLoS ONE 10(11): e0140474. doi: 10.1371/journal.pone. 0140474.
11. Potamitis I.; Rigakis I. (2015). Novel Noise-Robust Optoacoustic Sensors to Identify Insects through Wingbeats. IEEE Sensors Journal, 15, no.8, 4621, 4631, Aug. 2015, doi: 10.1109/JSEN.2015.2424924.
12. Potamitis I.; Rigakis I. (2016). Large Aperture Optoelectronic Devices to Record and Time-stamp Insects Wingbeats, IEEE Sensors Journal, 16, no. 15, pp. 6053-6061, Aug.1, doi: 10.1109/JSEN.2016.2574762.